PREDICTION OF BINDER POLYMERIZATION RATE IN THE GLASS WOOL CURING OVEN

Boris KRAŠEVEC[1], Yasir Beeran POTTA THARA[1,2], Hanuma Reddy TIYYAGURA [1,2], Simon MUHIČ[1,2,3]

[1] Faculty of Industrial Engineering Novo mesto, Šegova ulica 112, 8000 Novo mesto, Slovenia

[2] Rudolfovo - Science and Technology Center Novo mesto, Podbreznik 15, 8000 Novo mesto, Slovenia

[*3] Institute for Renewable Energy and Efficient Exergy Use, Cesta 2. grupe odredov 17, 1295 Ivančna Gorica, Slovenia

[*] Corresponding author; E-mail: simon.muhic@inoveks.si

Binder polymerization in the curing oven was investigated experimentally in the glass wool production. First focus was on the measurements of glass wool layer temperature distribution along the curing oven. The different temperature curves were compared with fibre density distribution in a layer of glass wool, measured with the x-ray device. The maximum difference between the temperature curves amounted to 60°C and fibre density distribution deviated for ±8 % according to nominal density. With a Near Infra-Red (NIR) spectroscopy binder polymerization rate was measured and compared with a set average temperature of curing oven, where the regression model was determined. With temperature reduction for 9 °C and polymerization rate decreasing for 2% were defined optimal product quality. In the next study, binder polymerization rate was predicted with aid of set temperatures and fan rotational frequency as input process parameters and Near Infra-Red spectroscopy as continuous response variable, where the temperature shown bigger impact than fan rotational frequency. Next prediction was done with aid of the input parameters and the magnitude of the fan rotational frequency and temperature as a response variable. In this case, the input quantities represent: a type of product, curing oven saturation, the ambient temperature, micronaire, area weight of the product and binder amount in the glass wool product. For each zone of the curing oven, an equation was determined to predict the magnitude of the fan rotational frequency and temperature. Regression models results showed high correlation with the determination coefficient r^2 higher than 0.85.

Key words*: Glass wool, curing oven, regression model, binder polymerization*

1. Introduction

Glass wool (GW) is one of the most widely utilized thermal insulation materials [1, 2]. Apart from GW, silicate materials are often used as thermal insulation coatings [3]. However, waste is produced as by-products of the production process and is considered to be impossible to recycle completely [4]. It is reported that about 800 000 tons of GW waste is produced in Europe every year and most of it are landfilled or unutilized [5]. The manufacturing process of GW includes the addition of raw materials, mainly trash glass, into the furnace followed by melting at a temperature of around 1300 °C. The stabilization channel receives the molten glass mixture before it is poured through the funnel and into the revolving spinners. Melt is extruded through spinner holes to generate fibers, which are subsequently coated with binder. The fibers are oriented downward toward the collecting chamber by the coaxial blow-away air flow with adjustable pressure and finally collected to form raw glass wools and then transported through the polymerization chamber, where the binder polymerisation process occurs.

The curing oven channel in the GW production process is a crucial part since it allows the smoke fumes to heat the glass wool and initiate the polymerization process. The binder polymerization process begins when the temperature of the glass wool layer rises over the activation temperature. GW contains about 5 to 10 wt.% of organic resin, often phenolic binder, and sugar-based binder to enable the operation [6]. While sugar-based binders are created by polycondensing naturally occurring plant-based components, phenolic binders are created via a polymerization reaction involving phenol, formaldehyde, and urea. The selection of resins is typically based on improving the processability and achieving desirable attributes including plasticization, coloring, and flame retardancy. It's crucial to understand that phenol-formaldehyde resin begins to break down during GW production at a temperature higher than 250 °C. At such temperatures, the binder begins to harden, resulting in successive lacing of fibres which provides characteristic mechanical properties such as tensile, compressive, and bending strengths [7]. Ducman *et* al. studied the influence of the curing regime and liquid-to-solid ratio utilized in glass wool and stone wool containing organic binder and detected superior mechanical properties in GW with organic binders [8]. Zhang and his team studied the mechanical properties of aluminate cement mortar mixed with chopped steel fibers and basalt fibers under high temperature and reported improved mechanical properties [9].

The curing oven enables continuous adjustment of layer thickness and velocity of the glass wool layer to achieve the desired specific density. Layer velocity must be corrected on a permanent basis due to interdependent factors such as layer thickness, specific mass, and conveyor belt velocity.

The single variable that affects glass wool capacity is conveyer belt velocity, which varies with layer thickness and density. The mass of the glass wool layer is measured to adjust the transporter velocity. The variable velocity impacts the retention period in the curing oven, which influences the bonding process. This influences the aero-thermodynamic properties of circulating smoke gases. The regulation of aero-thermodynamic variables in the polymerization process is crucial for ensuring the functionality of the production process and minimizing fuel consumption. Factors like circulation system sealing, smoked gas removal, and transporter perforations influence the formation of functional areas of transition velocity of smoked gases [10].

Industrial ovens significantly impact product quality, but energy consumption, complex thermo-physical processes, and monitoring difficulties pose challenges. Yuan Yi et al. improved

curing cycle time in industrial continuous convection ovens by numerically modeling air flow. They found that higher line speed reduces product temperature, and higher airflow velocities increase it [11]. Several experimental and numerical studies focused on optimizing a curing oven, focusing on uniform temperature, optimal pressure, sensitive products, energy loss minimization, insulation use, internal air flow balance, and temperature optimization using simulation [12–14]. Yüksel *et* al. proved that the effective thermal conductivity of GW reinforced aluminium samples increases uniformly with increasing the temperature [15]. The addition of extra layers in samples reduces effective thermal conductivity at low temperatures, resulting in improved insulation.

The quantity of waste glass wool has to be reduced from the production cost reason and the environmental side. One of the main reasons for the waste glass wool material is polymerization process. If will be well described and understood, then glass wool production would drive the process more optimal and make value added to the productivity and environment.

The current study evaluates the temperature characteristics of glass wool layers as they progress through the curing oven. The fiber density distribution in a layer of glass wool was studied with x-ray equipment, and the binder polymerization rate was determined using near infrared (NIR) spectroscopy. The binder polymerization rate was predicted using varied fan rotational frequency and temperature settings per curing oven zone. The regression model employed the kind of glass wool product, saturation, ambient temperature, micronaire, binder content, and fan rotational frequency to forecast the fan rotational frequency and temperature in each zone of the curing oven.

2. Methods

For better understanding of polymerization process the measurements of glass wool layer temperature characteristics along the curing oven were performed, fiber density distribution in a layer of glass wool was studied and binder polymerization rate (NIR) was analysed.

2.1. Measurements of glass wool layer temperature characteristics along the curing oven

One of the important diagnostic parameters is also the knowing of temperatures in the glass wool layer at its transition through the curing oven. According to the possibilities of local temperature changes in the layer, periodical temperature measurement in the glass wool layer turns out to be the appropriate method. This method requires the implementation of a thermo isolated PC unit (Fig. 1) with six connected thermocouples. The isolation of the PC unit prevents the temperature in the unit to rise above the allowed 70 °C while the measurements of glass wool transition through the curing oven are performed. The installation scheme for the implementation of the measuring system is shown in Figure 2. The installed experimental equipment is moving together with the glass wool layer through the curing oven. During this, the current measured temperature values captured by particular sensors are saved on the PC. Because the movement velocity along the oven is constant during the experiment, the longitudinal position of the curing oven according to the measured local temperatures in the glass wool layer is also clearly determined.

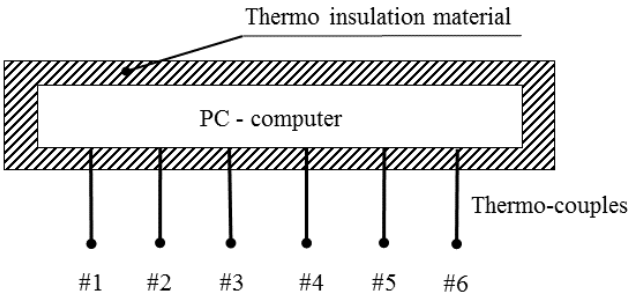

Fig. 1. Process unit, type Q18 for continuous capturing of local temperatures in the glass wool layer

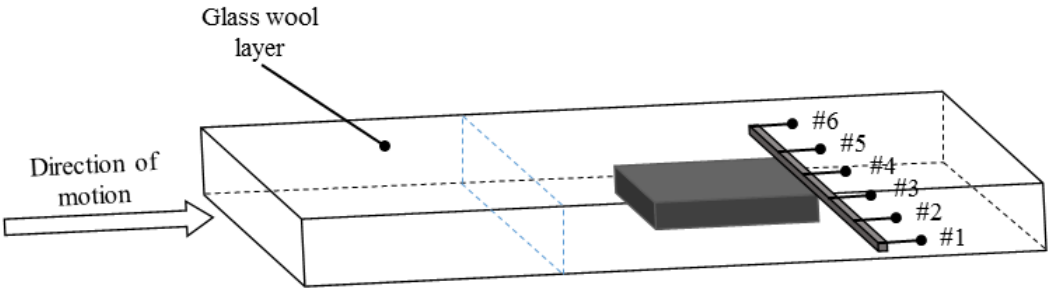

Fig. 2. Arrangement of temperature sensors in the glass wool layer

Figure 3 represents the function scheme of flow of smoke gases passing through the glass wool layer. The displayed segment includes the basic components which are present in a real polymerisation process.

Glass wool layer continuously enters the curing oven which consists of two separated areas. These two areas are separated by a layer of glass wool that is located between two perforated conveyor belts which are moving together with the layer through the oven. The pressure difference is generated by the circulation fan that moves the smoke gases through the glass wool layer. At a given functional velocity of smoke gases, the pressure difference depends on the aerodynamic-resistive characteristics of glass wool. Smoke gases from the oven area of negative pressure enter the gas burner where they are heated up by the combustion of fuel and controlled supply of air necessary for the combustion. The circulation fan transports the heated smoke gases into the lower chamber with overpressure. At nominal volume rate of flow, this fan must overcome the pressure losses in the circulation system and the aerodynamic losses that occur when the smoke gases pass through the glass wool layer. Since the fuel combustion in the combustion chamber supplies the sufficient energy to heat up the glass wool layer and polymerise the binder, the quantity of smoke gases in the circulation system increases. The generated quantity of smoke gases mostly depends on the amount of fuel, supplied air and water that evaporates when the layer is heated up. To remove the smoke gases, the negative pressure circulation system is connected to the suction fan. This fan sustains the stationary pressure conditions in the circulation system and transports the redundant smoke gases into the system of smoke gas combustion and further through the filters into the atmosphere. The operating regime of the suction fan depends on pressure conditions in the circulation system and on the amount of newly formed smoke gases. Usually, the operating point of this fan is adaptively set so that the absolute pressure in the smoke gases is the same as the pressure in the atmosphere where the smoke gases are

passing through the glass wool layer. This ensures the minimal transition of smoke gases into the environment and optimal fuel consumption [10].

The oven in our case is divided into nine zones with exchanging direction of circulation flows. The number of zones is dependent from product area weight and power of fans. In the first five zones, the pressure in the upper area (position 1, Fig. 3) is lower than the pressure in the bottom area of the oven (position 2, Fig. 3). Opposite situation is in last four zones.

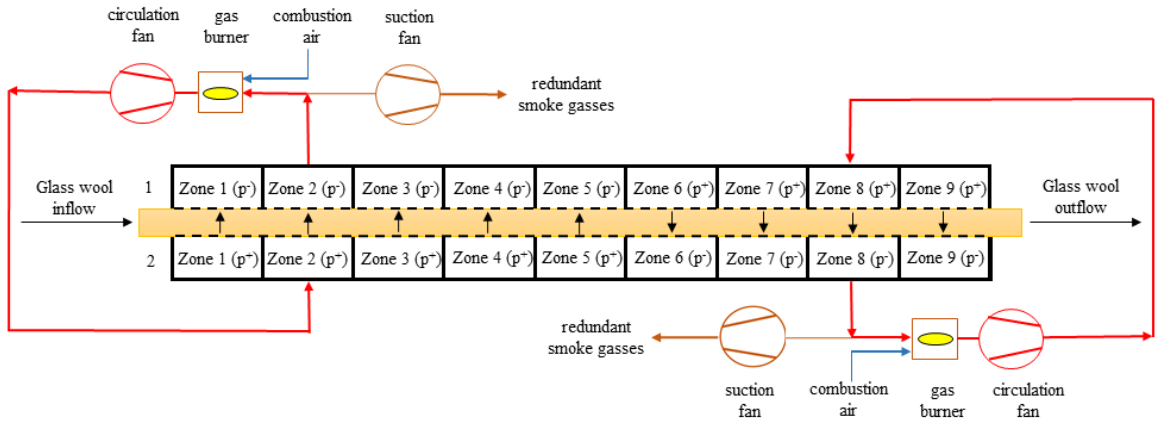

Fig. 3. Functional scheme of the curing oven

Table 1 presents four operating points by constant fan rotational frequency (n) and changes only by temperature (T) per curing oven zone. To stabilize the temperature in the polymerization chamber, the experiments were performed at two-hour intervals. Glass wool samples were taken for measuring the degree of polymerization (NIR) by each operating point. During the test, fiber density distribution in a layer of glass wool was measured with an x-ray device. Temperature profiles in the polymerization chamber were measured using calibrated thermocouples and a data logger device, type Q18 with an accuracy of ± 0.5 °C. Glass wool line speed was 36 m/min and product area weight 1.3 kg/m^2.

Table 1. Setting parameters by curing oven zones. The temperature is described with T_1 – T_9, while n_1 – n_9 represents the fan rotational frequency.

Op. point no.	T_1 (°C)	T_2 (°C)	T_3 (°C)	T_4 (°C)	T_5 (°C)	T_6 (°C)	T_7 (°C)	T_8 (°C)	T_9 (°C)
1	240	245	250	260	270	275	280	280	275
2	230	230	240	250	260	270	270	270	275
3	280	260	230	230	230	250	260	260	250
4	255	275	240	225	225	240	240	250	250

Op. point no.	n_1 (min^{-1})	n_2 (min^{-1})	n_3 (min^{-1})	n_4 (min^{-1})	n_5 (min^{-1})	n_6 (min^{-1})	n_7 (min^{-1})	n_8 (min^{-1})	n_9 (min^{-1})
1	400	350	350	300	300	300	300	350	350
2	400	350	350	300	300	300	300	350	350
3	400	350	350	300	300	300	300	350	350
4	400	350	350	300	300	300	300	350	350

Operating point 1 represents the standard temperature and fan rotational frequency settings. In operating point 2, the temperatures were reduced to 9 °C on average. In operating point 3, the temperatures were additional decreased compared to operating point 2. Only in zones 1 and 2 did the temperatures increase with the assumption of faster water evaporation and consequently early polymerization beginning. In operating point 4, temperatures were reduced by 6 °C on average related to the test 3. According to operating point 3, the temperatures in zone 1 and zone 2 were set opposite. The lower value was set in zone 1 and higher in zone 2.

Figure 4 presents the results of glass wool temperature measurements. The results are calculated to a longitudinal position in the oven. That enables the connection of local temperatures with local particularities inside the oven. Position 1 in the chart legend presents glass wool temperature on the right side of transporter belt moving and position 6 left side (Fig. 2). The vertical gray continuous lines in the diagrams marked from 1 to 6 indicate the first 6 zones in the curing oven. The diagram in Figure 4 describes the temperature of the glass wool at operating point 2.

Data logger device starts showing value at 18 °C. That presents ambient temperature. Measuring device in the glass wool shows 30 °C, which is before curing oven. After that all 6 curves were increased to 60 °C where the polymerization begins. That is happening at the beginning of the third zone. From here, the curves rise intensively to zone 6 and continue slightly to the end of the curing oven, where the glass wool reaches from 190 °C to 210 °C.

Similar temperature curve shapes were obtained at all four operating points. Differences were observed at operating point 3, when we increased the temperatures in zones 1 and 2. Due to the increase in temperatures, the temperature of the glass wool previously reached 60 °C, but the polymerization started not earlier. In operating point 4, a lower temperature was set in zone 1 and a higher temperature in zone 2. The shape of the temperature curves in the glass wool has not changed. Consequently, 230 °C can be determined as the optimal temperature for the first two zones.

The curves of temperature here differ from each other. This implies that the glass wool is non-homogenous. Local non-homogeneities of glass wool are local specific density, presence of non-homogenous binder distribution and humidity part.

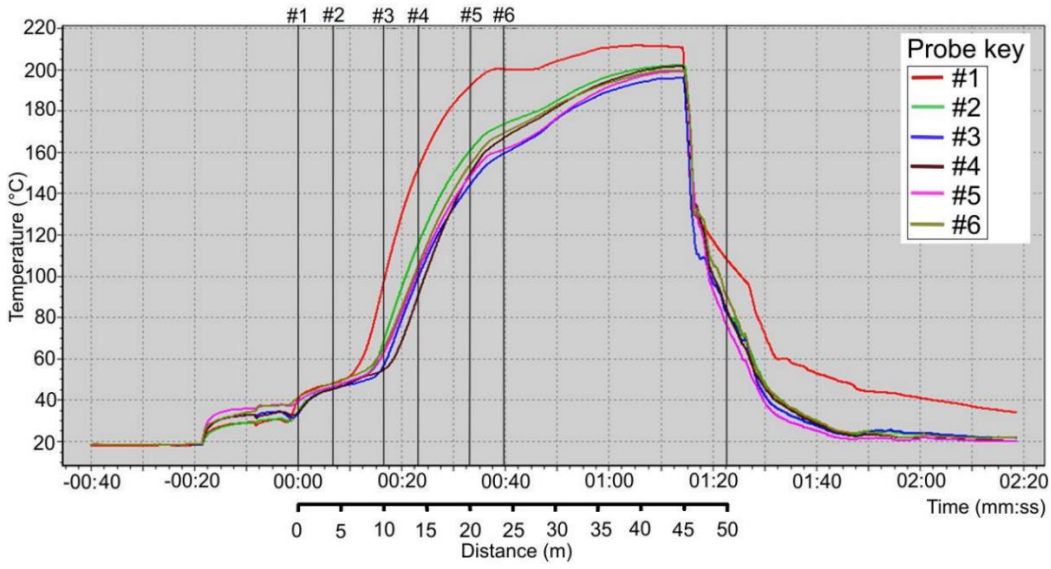

Fig. 4. Temperature distribution in the glass wool layer along the curing oven

2.2. Fiber density distribution in a layer of glass wool

The x-ray device works on a non-contact principle. Above the device main structure, a radiation source is located while the radiation detector is placed below the line belt. The x-ray radiation from the source penetrates the measured material and is partly absorbed in it, depending on the quantity and specific weight of the analyzed material. The unabsorbed radiation component is picked up by the detectors and converted into electrical signals for further evaluation.

The absorption is given by Equation 1:

$$I = I_0 \cdot e^{-\mu_m \rho x} \tag{1}$$

In Equation 1, I is the remaining radiation intensity after passing through the material of thickness x, I_0 is the intensity of the radiation before entering into the material, μ_m [m^2/kg] the mass attenuation coefficient of the material and ρ [kg/m^3] the raw density of the material. The mass attenuation coefficient is a material attribute which depends on the chemical composition of the material. The area weight f [kg/m^2] can be calculated directly from the corrected intensity values (Eq. 2).

$$f = \frac{log\left(\frac{I_0}{I}\right)}{\mu_m} \tag{2}$$

From the area weight f and the material thickness x, the raw density (Eq. 3) is calculated [5, 11]:

$$\rho = \frac{f}{x} \tag{3}$$

Figure 5 presents fibre density distribution in period when all four glass wool temperature measurements were performed. Fibre density distribution was measured with the x-ray measurement device with a spatial resolution of 300x300 mm and is described with ±8 % deviation according to nominal density value.

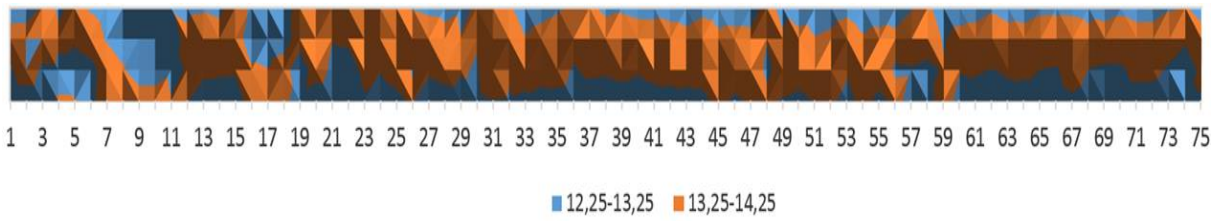

Fig. 5. Fibre density distribution in a layer of glass wool

2.3. Binder polymerization rate (NIR)

Near Infra-Red spectroscopy is an analysis method that uses the NIR region of the electromagnetic spectrum (800 – 2500 nm). It measures the absorption of light from the sample in the NIR region at different wavelengths. The recorded NIR spectrum consists of overtones and combination vibrations of molecules that contain CH, NH or OH groups. When light is reflected from solid surfaces or particles in powders, pellets or granulates, it is called diffuse reflection (Fig. 6). In an integrating sphere light is directed in a broad nearly parallel beam onto a sample. The diffusely reflected light is well distributed in the sphere by multiple diffuse reflections at the gold-plated inner

surface, homogenizing the light. Therefore, an integrating sphere is well suited for inhomogeneous samples as well as for fine powders. Depending on the sample, light may penetrate beyond the surface a significant distance, e.g. for powders its approx. 2 to 4 mm depending on particle size, wavelength, and density, thus enabling the quantification of components within the sample [16].

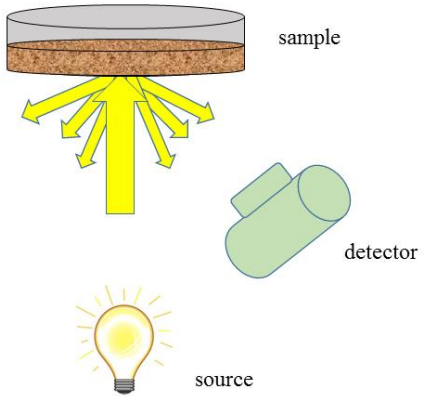

Fig. 6. Near Infra-Red spectroscopy (NIR)

Glass wool samples were taken at three points in the transverse direction of the production line. Each sample was splitted into three equal parts by glass wool height and was used on a NIR device to determine the degree of polymerization of the binder. According to experience, optimal polymerization rate of the binder is estimated at 80 ± 2 %.

Curing oven fans from zone 6 to zone 9 transports hot air on the upper side of glass wool. Temperatures in operating point 1 are used from experience and confirms 79.2 % polymerization of glass wool. Excessive temperature settings are in zones 1 to zone 5, which is confirmed by NIR measurements (88.7 %). In these zones, the fans transfer hot air to the glass wool from the bottom side.

Table 2. Average temperature and polymerization rate for four operating point

Op. point no.	Average *T* (°C)	NIR (%) (average)	NIR (%) (up)	NIR (%) (bottom)	NIR (%) (middle)
1	264	83.6	79.2	88.7	83.0
2	255	81.6	78.0	85.5	81.3
3	250	77.3	74.1	81.6	76.1
4	244	76.7	73.4	81.2	75.6

The average temperature, decreased by 9 °C at operating point 2, shows a reduction in the polymerization at the upper, middle, and bottom level from 1.2 % to 3.2 % and present optimal polymerization rate. Temperatures in operating point 3 and 4 were reduced too much, indicating an average measurement of NIR with polymerization below 78 %. Average temperature and average polymerization are in good correlation, what is confirmed by a high value of determination coefficient, $r^2 = 0.91$, indicating good quality of regression modelling (Eq. 4):

$$NIR = -15.8 + 0.3776 \cdot Average\ T \quad (4)$$

3. Results and discussion

The experiments were conducted in the curing oven in a real production process. More than one hundred experiments were performed at different fan rotational frequency and temperature per curing oven zone. Binder polymerization was measured by each operating point. Production process parameters were set in such manner that the product quality was adequate for packaging and sale, hence all measured variables corresponded to a set of real production parameters.

Table 3. Setting parameters by curing oven zones. The temperature is described with T_1 – T_9, while n_1 – n_9 represents the fan rotational frequency. Binder polymerization is described with calculated and measured NIR value.

Op. point no.	T_1 (°C)	T_2 (°C)	T_3 (°C)	T_4 (°C)	T_5 (°C)	T_6 (°C)	T_7 (°C)	T_8 (°C)	T_9 (°C)	Measured *NIR* (%)
1	255	260	265	270	270	270	270	270	260	83.4
2	265	265	270	270	270	270	280	280	275	86
3	260	270	270	270	270	270	270	280	260	84.6
4	260	260	260	270	270	280	280	270	270	85.5
…	…	…	…	…	…	…	…	…	…	…
110	250	255	260	260	270	270	265	260	260	80
111	260	260	265	270	275	280	275	275	270	80.6
112	260	260	265	270	275	280	275	270	265	81.3
113	255	260	260	270	270	270	270	260	260	80.4

Op. point no.	n_1 (min^{-1})	n_2 (min^{-1})	n_3 (min^{-1})	n_4 (min^{-1})	n_5 (min^{-1})	n_6 (min^{-1})	n_7 (min^{-1})	n_8 (min^{-1})	n_9 (min^{-1})	Calculated *NIR* (%)
1	500	550	550	600	600	600	600	600	600	82.9
2	650	700	700	800	800	900	900	800	700	85.7
3	550	600	650	700	750	650	600	550	500	84.6
4	600	700	850	900	950	900	850	800	800	83.7
…	…	…	…	…	…	…	…	…	…	…
110	400	400	450	450	400	400	400	400	400	78.8
111	400	400	400	400	350	350	350	350	350	79.7
112	600	550	600	650	600	550	550	600	600	81.2
113	450	500	500	500	500	500	500	500	450	80.5

A good correlation is expected between the binder polymerization rate (*NIR*, Table 3) and the process input parameters ($T_{1\text{-}9}$, $n_{1\text{-}9}$, Table 3). This hypothesis will be confirmed by the following linear regression model:

$$y = b_0 + b_1X_1 + b_2X_2 + \cdots + b_kX_k \quad (5)$$

In regression Equation 5, the y is the continuous response variable (NIR), b_0 is the constant, b_1, b_2, ..., b_k are the coefficients, X_1, X_2, ..., X_k are the values of the terms (temperatures and fan rotational frequency). Values of regression model constants are presented in Table 4. Parameters with negative

values inversely influence the binder polymerization rate. Their significance was checked with a *t*-test (Table 4).

Table 4. Regression model coefficients values with the results of the t-test

	b_0	b_1	b_2	b_3	b_4	b_5	b_6	b_7	b_8	b_9
Values	85.58	0.1115	- 0.0635	- 0.0582	0.0199	0.0007	- 0.0676	- 0.0040	0.1589	- 0.1257
Prob >|t|		0.548	0.554	0.514	0.493	0.510	0.577	0.702	0.752	0.685

	b_{10}	b_{11}	b_{12}	b_{13}	b_{14}	b_{15}	b_{16}	b_{17}	b_{18}
Values	0.003267	- 0.00115	- 0.00952	- 0.00633	0.01164	0.00334	0.00584	- 0.00018	0.00002
Prob >|t|	11.8	11.1	11.7	13.6	14.7	15.1	14.1	13.3	11.1

The results presented in Table 4 show the parameter impact on the binder polymerization rate. Parameters b_1 - b_9 present the temperatures in curing oven zones and have the biggest impact on the binder polymerization rate. Smaller impact results from the rotational frequency of fans (parameters b_{10} - b_{18}) used for circulation hot air through the glass wool.

The comparison between measured NIR and the ones calculated based on regression model is shown in Figure 7. A good agreement between calculated and measured values *NIR* is confirmed by a high value of determination coefficient, r^2 = 0.88, indicating good quality of regression modelling. Equation 6 describe correlation between measured and calculated NIR value:

$$\text{Calculated } NIR = 6.347 + 0.921 \cdot \text{Measured } NIR \quad (6)$$

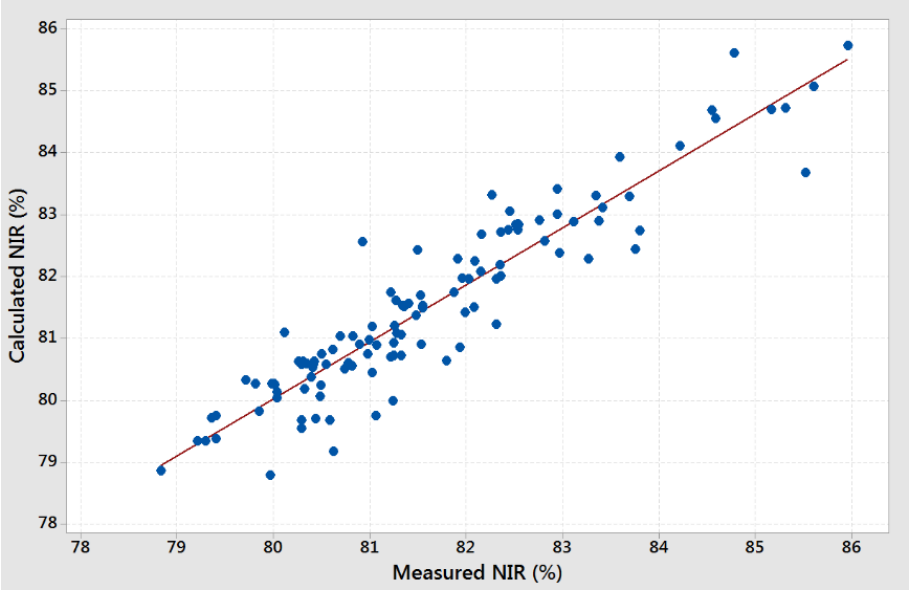

Fig. 7. Correlation between measured and calculated values of NIR (r^2 = 0.88)

So far, we have focused on the correlation of fan rotational frequency and temperature with respect to the rate of *NIR* polymerization. The connection between the input parameters and the magnitude of the fan rotational frequency and temperature as a response variable is presented below. For each zone of the curing oven, an equation was determined to predict the magnitude of the fan rotational frequency and temperature. In this case, the input quantities represent:

- A type of product where light rolls is marked LR (1), heavy rolls HR (2), light plates LP (3) and heavy plates HP (4).
- Saturation: Every two months, fibers are removed from the curing oven. Broken fibres saturate curing oven interior during the polymerization process and represent a certain resistance to the circulation of hot air. In the regression model, the time after curing oven interior cleaning, ranged from 1 to 60 days, was taken into calculation.
- The ambient temperature depends on the season. Calendar year we divided into three parts, where the coldest ambient temperatures present wintertime (10), the warmest temperatures are on the summertime (30), and we combined spring and autumn time, where ambient temperatures are similar (20).
- Micronaire (MIC) is a measure of the air permeability of compressed glass wool fibers and is used as an indicator of fibre fineness. The micronaire presented in Table 5 ranges between 2.86 and 3.24. The dependence of the micronere on the fiber diameter and the standard deviation (SD) is described by Equation 7 [17]:

$$MIC = 1.7940 + 0.1177 \cdot \text{fibre diameter} + 0.0633 \cdot \text{SD of fibre diameter} \quad (7)$$

- Area weight of the product a, where ρ is the density and h are the thickness of the glass wool (Eq. 8). The area weight presented in Table 5 is ranged between 0.68 and 4.4 kg/m^2.

$$a = \frac{\rho}{h} \quad (8)$$

- The binder represents 4.6 to 6.6 % of the material content in the product.

Table 5 present values of 52 experiments performed at different types of glass wool product, saturation, ambient temperature, micronaire and fan rotational frequency of zone 5.

Table 5. Rotational frequency of zone 5 as continuous response variable and values of the terms (type of product, saturation, ambient temperature, micronaire, product area weight, binder content)

Op. point no.	Type of product; LR (1), HR (2), LP (3), HP (4)	Saturation (day)	Ambient temperature (°C)	Micronaire (/)	Area weight (kg/m^2)	Binder (%)	*n* of zone 5 (min^{-1})
1	1	40	30	3.00	1.05	4.6	300
2	2	46	30	3.10	1.55	5.6	450
3	4	4	30	2.88	2.00	6.6	600
4	1	35	20	3.20	0.98	4.6	250
…	…	…	…	…	…	…	…
49	3	45	20	2.96	2.15	5.6	500
50	2	14	10	2.90	4.80	5.6	650
51	1	56	20	2.86	1.35	4.6	400
52	4	60	20	3.14	2.00	6.6	550

In the regression Equation 5, the y is the continuous response variable (rotational frequency of zone 5), b_0 is the constant, b_1, b_2, ..., b_k are the coefficients, X_1, X_2, ..., X_k are the values of the terms (type of product, saturation, ambient temperature, micronaire, product area weight, binder content). Values of regression model constants are presented in Table 6. Parameters with negative values

inversely influence the binder polymerization rate. Their significance was checked with a t-test and *P* value (Table 6).

Table 6. Regression model coefficients values with the results of the t-test and P value

	b_0	b_1	b_2	b_3	b_4	b_5	b_6
Values	1003	19.2	0.703	1.69	- 368.8	49.27	64.7
Prob >|t|		0.168	2.58	1.04	0.0130	0.129	0.111
P value		0.047	0.017	0.013	0.001	0.001	0.034

The results presented in Table 6 show the parameter impact on the rotational frequency of zone 5. Parameter b_4 presents the micronaire and has the biggest impact on the rotational frequency of zone 5. Also important are the parameters b_1, b_5 in b_6 which present a type of product, area weight and binder. The smallest impact results from the ambient temperature and saturation (parameters b_2 and b_3). The probability (*P* value) that this hypothesis is valid was below 0.05, thus the regression is very significant.

The comparison between set and calculated values of rotational frequency on the basis of regression model is shown in Figure 8. A total of 52 experiments were performed at different types of glass wool product, saturation, ambient temperature, micronaire, product area weight, binder, and rotational frequency of zone 5. A good agreement between set and calculated values is confirmed by a high value of determination coefficient, $r^2 = 0.89$, indicating good quality of regression modelling.

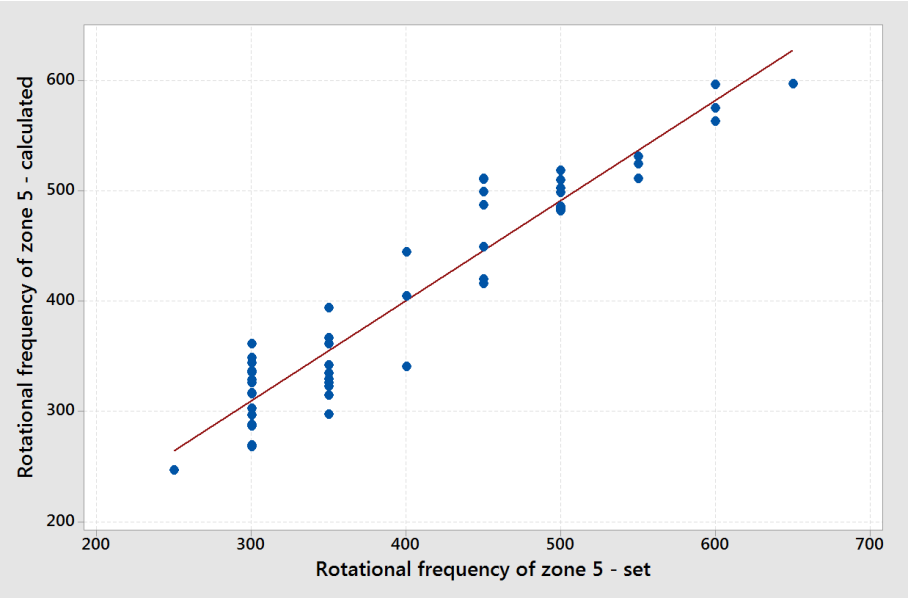

Fig. 8. Correlation between set and calculated values of rotational frequency ($r^2 = 0.89$)

4. Conclusions

The measurements of temperature distribution in the glass wool layer along the curing oven were performed. We measured the maximum temperature in the glass wool, determined the intensity of the temperature rise and started binder polymerization. Temperature sensors were located differently in the transverse direction of the curing oven and measured different temperature values. The curves of temperature here differ from each other. This implies that the glass wool is non-

homogenous. Local non-homogeneities of glass wool are local specific density, presence of non-homogenous binder distribution and humidity part.

The fibre density distribution in a layer of glass wool was measured with an x-ray device and compared with different temperature curves. The results show that lower density coincides with a higher temperature of the glass wool fibres. The maximum difference between the temperature curves amounted to 60°C and fibre density distribution deviated for ±8 % according to nominal density. With a Near Infra-Red spectroscopy was measured binder polymerization rate and compared with a set average temperature of curing oven, where the regression model was determined. With temperature reduction for 9 °C and polymerization rate decreasing for 2% were defined optimal product quality. Another prediction of binder polymerization rate was done with aid of set temperatures and fan rotational frequency as input process parameters and Near Infra-Red spectroscopy as continuous response variable, where the temperature shown bigger impact than fan rotational frequency. Next prediction was performed specially for the operators on the curing oven. For each zone of curing oven, an equation was determined to predict the magnitude of the fan rotational frequency and temperature. When the operator in the excel table enter a type of product, curing oven saturation, the ambient temperature, micronaire value, product area weight and binder content in the glass wool product, the prediction equation for each zone of the curing oven calculate the proper set temperature and fan rotational frequency, with which an optimal binder polymerization is achieved. Regression models results showed high correlation with the multiple regression coefficient r^2 higher than 0,85.

Further research in this area should include finite element (FE) simulations which exclude possible material fatigue or other mechanical problems. Warm outgoing smoke gases can be redirected again into the dryer or to another step in the process. Focus on adaptively set fan, so that the absolute pressure in the smoke gases is the same as the pressure in the atmosphere where the smoke gases are passing through the glass wool layer. This ensures the minimal transition of smoke gases into the environment and optimal fuel consumption.

References

[1] Yliniemi, J., et al., Mineral Wool Waste-Based Geopolymers, *IOP Conf. Ser. Earth Environ. Sci.*, *297* (2019), 1, pp. 012006

[2] Padmanaban, G., et al., Performance Of A Desiccant Assisted Packed Bed Passive Solar Dryer For Copra Processing, *Therm. Sci.*, *21* (2017), pp. 419-426

[3] WEI, C., et al., Development Of A New Silicate Thermal Insulation Coating And Analysis Of Heat Storage Characteristics, *Therm. Sci.*, *27* (2023), 2, pp. 949-957

[4] Luukkonen, T., et al., One-Part Alkali-Activated Materials: A Review, *Cem. Concr. Res.*, *103* (2018), pp. 21-34

[5] Lemougna, P.N., et al., Utilisation Of Glass Wool Waste And Mine Tailings In High Performance Building Ceramics, *J. Build. Eng.*, *31* (2020), pp. 101383

[6] Lemougna, P.N., et al., Effect Of Organic Resin In Glass Wool Waste And Curing Temperature On The Synthesis And Properties Of Alkali-Activated Pastes, *Mater. Des.*, *212* (2021), pp. 110287

[7] Bennett, T.M., et al., Low Formaldehyde Binders For Mineral Wool Insulation: A Review, *Glob. Challenges*, *6* (2022), 4, pp. 2100110

[8] Pavlin, M., et al., Mechanical, Microstructural And Mineralogical Evaluation Of Alkali-Activated Waste Glass And Stone Wool, *Ceram. Int.*, *47* (2021), 11, pp. 15102-15113

[9] Xu, P., et al., Experimental Study On High Temperature Mechanical Properties Of Aluminate Cement Mortar Mixed With Fiber, *Therm. Sci.*, *25* (2021), 6, pp. 4441-4448

[10] Širok, B., et al., *Fiberisation Process*, Woodhead Publishing, 2008

[11] Yi, Y., et al., Improving The Curing Cycle Time Through The Numerical Modeling Of Air Flow In Industrial Continuous Convection Ovens, *Procedia CIRP*, *63* (2017), pp. 499-504

[12] Pask, F., et al., Systematic Approach To Industrial Oven Optimisation For Energy Saving, *Appl. Therm. Eng.*, *71* (2014), 1, pp. 72-77

[13] Pask, F., et al., Industrial Oven Improvement For Energy Reduction And Enhanced Process Performance, *Clean Technol. Environ. Policy*, *19* (2017), 1, pp. 215-224

[14] Carvalho, M.D.G., Nogueira, M., Improvement Of Energy Efficiency In Glass-Melting Furnaces, Cement Kilns And Baking Ovens, *Appl. Therm. Eng.*, *17* (1997), 8-10, pp. 921-933

[15] Yüksel, N., et al., The Temperature Dependence Of Effective Thermal Conductivity Of The Samples Of Glass Wool Reinforced With Aluminium Foil, *Int. Commun. Heat Mass Transf.*, *37* (2010), 6, pp. 675-680

[16] Cendre, E., et al., Conception Of A High Resolution X- ray Computed Tomography Device; Application To Damage Initiation Imaging Inside Materials, (1999)

[17] Kraševec, B., et al., Multiple Regression Model Of Glass Wool Fibre Thickness On A Spinning Machine, *Glas. Technol.*, *55* (2014), 4, pp. 119-125

Paper submitted: 24.02.2024.

Paper revised: 30.03.2024.

Paper accepted: 05.04.2024.